Journal of Materials Chemistry C

Bis(4-dialkylaminophenyl)heteroarylamino donor chromophores exhibiting exceptional hyperpolarizabilities

Journal:	*Journal of Materials Chemistry C*
Manuscript ID	TC-ART-12-2020-005700.R1
Article Type:	Paper
Date Submitted by the Author:	02-Feb-2021
Complete List of Authors:	Xu, Huajun; University of Washington Johnson, Lewis; University of Washington, Chemistry; Nonlinear Materials Corporation de Coene, Yovan; Katholieke Universiteit Leuven, Department of Physics and Astronomy Elder, Delwin; University of Washington, Department of Chemistry Hammond, Scott; University of Washington; Nonlinear Materials Corporation Clays, Koen; KU Leuven, Chemistry Dalton, Larry; University of Washington, Department of Chemistry Robinson, Bruce H.; Univ Washington, Chemistry

Bis(4-dialkylaminophenyl)heteroarylamino donor chromophores exhibiting exceptional hyperpolarizabilities†

Huajun Xu,[a] Lewis E. Johnson,[*ab] Yovan de Coene,[cd] Delwin L. Elder,[*a] Scott. R. Hammond,[ab] Koen Clays,[c] Larry R. Dalton,[a] Bruce H. Robinson[a]

*Corresponding authors (L.E.J: lewisj@uw.edu, D.L.E.: elderdl@uw.edu)

Abstract

Organic electro-optic (EO) materials incorporated into silicon-organic hybrid and plasmonic-organic hybrid devices have enabled new records in EO modulation performance. We report a new series of nonlinear optical chromophores engineered by theory-guided design, utilizing bis(4-dialkylaminophenyl)heteroarylamino donor moieties to greatly enhance molecular hyperpolarizabilities. Hyperpolarizabilities predicted using density functional theory were validated by hyper-Rayleigh scattering measurements, showing strong prediction/experiment agreement and > 2-fold advancement in static hyperpolarizability over the best prior chromophores. Electric field poled thin films of these chromophores showed significantly enhanced EO coefficients (r_{33}) and poling efficiencies (r_{33}/E_p) at low chromophore concentrations compared with state-of-the-art chromophores such as **JRD1**. The highest performing blend, containing just 10 wt% of the novel chromophore **BTP7**, showed a 12-fold enhancement in poling efficiency per unit concentration vs **JRD1**. The results suggest that further improvement in chromophore hyperpolarizability is feasible without unacceptable tradeoffs with optical loss or stability.

† Electronic supplementary information (ESI) available: Synthetic procedures and analytical, UV/visible spectra in a variety of solvents, variable angle spectroscopic ellipsometry (VASE) data for films of chromophores and chromophore-polymer blends, poling data (plots of r_{33} vs. poling field), glass transition temperatures (T_g) as determined by differential scanning calorimetry (DSC), decomposition temperatures (T_d) as determined by thermogravimetric analysis (TGA), HRS data analysis, computational methodology, cyclic voltammetry methods and data, and FTIR methods and data. See DOI:

[a] *University of Washington Department of Chemistry, Seattle WA 98195, USA*.

[b] *Nonlinear Materials Corporation, Seattle WA 98109, USA.*

[c] *Department of Chemistry, University of Leuven, Celestijnenlaan 200D, 3001 Leuven, Belgium.*

[d] *Department of Physics and Astronomy, University of Leuven, Celestijnenlaan 200D, 3001 Leuven, Belgium.*

Introduction

Renewed interest in organic electro-optic (OEO) materials has recently been witnessed due to record-setting demonstrations in silicon-organic hybrid (SOH) and plasmonic-organic hybrid (POH) devices,[1-16] which combine the high intrinsic electro-optic activity of organic chromophores[17-19] with the tight confinement and improved overlap of electrical and optical fields achievable in nanophotonic devices, enabling chip-scale integration with CMOS electronics.[5, 20] State-of-the-art hybrid inorganic/organic modulator systems have already demonstrated ultra-high electro-optical bandwidths greater than 500 GHz,[5] energy efficiencies ≤ 70 aJ/bit,[10, 21] small device footprints < 10 μm^2, and voltage-length parameters ($V_\pi L$) of ≤ 50 V-μm with existing high-performance OEO materials.[15, 16] To achieve $V_\pi L$ values < 10 V-μm (critical for low insertion loss, best energy efficiency, and the highest bandwidth operation), hybrid inorganic/organic modulators require novel device designs and engineering as well as improved EO activity.[2, 22, 23] OEO material performance ultimately depends on a combination of chromophore hyperpolarizability (β), electric field poling-induced acentric order of the chromophores ($<\cos^3\theta>$), chromophore number density (ρ_N), and the refractive index of the material (*n*) at the operational wavelength. EO activity of organic materials is proportional to the molecular β, which can be tuned by the donor—π bridge—acceptor structure of the molecule. While bulk and in-device EO activity has been improving[2, 24] due to improving ordering via side-chain engineering, chromophore blending, and increasing chromophore number density, β has not increased significantly in about a decade. This is partly because the absorbance in the near-IR generally increases as β increases, thus increasing optical loss of higher β materials; which has often resulted in too large of a tradeoff versus EO activity. However, hybrid device designs with sub-mm path lengths are less sensitive to propagation loss, and theory-aided design can be utilized to mitigate loss/EO activity tradeoffs.[2, 25] We have used a theory-guided design process including quantum mechanical and statistical mechanical techniques to design a new generation of OEO materials relevant to hybrid devices.[2, 25, 26] The combination of experimental and theoretical studies affords better understanding of structure-property relationships, as well as the prospects for implementation in nanoscale photonic devices.[26]

We report a series of chromophores with enhanced β and *n* that are derived from powerful bis(4-dialkylaminophenyl)heteroarylamino electron donating groups. OEO molecules with bis(4-alkoxyphenyl)arylamino or bis(4-alkoxyphenyl)heteroarylamino donors have previously been demonstrated by Cheng et al. and Davies et al.;[27, 28] chromophores based on these donors showed increased hyperpolarizability, but bulk electro-optic activity of these materials lagged behind other contemporary approaches such as dendrimers[29-32] and binary chromophore organic glasses.[33-35] Our new designs leverage recent advances in theory-driven chromophore development to utilize even more powerful donor moieties in stable structures. Key to increasing β is balancing the aromaticity of the π bridge with the strength of the electron donor. Too much bridge aromaticity suppresses β, while too little aromaticity leads to an excessive redshift and formation of highly polar and difficult to process materials with zwitterionic ground states (ZGS), analogous to the two-state model behavior of donor-acceptor polyenes.[36] Instead of the phenyl ring in the common aminophenyltetraene bridge (see **YLD124** and **JRD1** in Figure 1), we chose the thieno[3,2-b]thiophene moiety to build the donor side of the chromophores in order to deliver increased stabilization of neutral ground state (NGS) character instead of monoheterocycles (e.g. thiophene or alkylpyrrole), which have shown a shift to ZGS character in more polar solvents.[27] The generic structure for these novel chromophores is shown in Scheme 1.

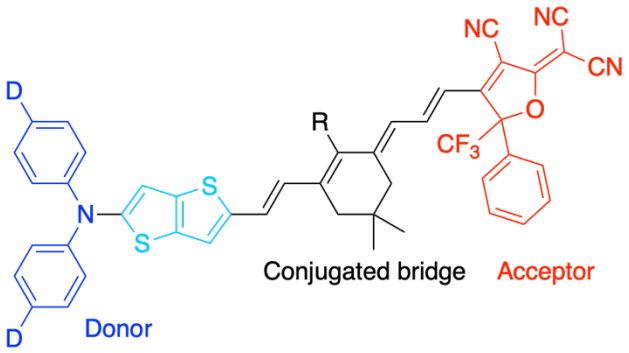

Scheme 1. Generic structure of a "**BTP**" (bisarylamine-thienothiophene-polyene) chromophore, showing the donor, bridge, and acceptor (top). The thienothiophene linkage in the donor, which provides enhanced stabilization of the neutral ground state is highlighted in light blue. Additional electron-donating moieties on the donor are labeled as D and the exposed conjugated site on the isophorone group within the bridge is labeled as R.

Results and discussion

Chromophores were modeled using density functional theory (DFT) at the M062X/6-31+G(d) level of theory, which provides accurate prediction of relative hyperpolarizabilities, as part of a large-scale computation and theory-driven search[25, 37, 38] for novel designs that would enhance hyperpolarizability while keeping dipole moment and band gap within acceptable constraints. We synthesized three different variants of the "**BTP**" structure shown in Scheme 1 that had different degrees of substitution with bulky *tert*-butyldiphenylsilyl (TBDPS) groups. **BTP3** lacks any TBDPS groups, **BTP5** is substituted with one pendant TBDPS off the electron donor, and **BTP7** additionally includes a pendant group off the bridge. These bulky groups improve solubility and processibility and can improve EO performance in many cases by discouraging chromophore aggregation (site isolation) and enabling more efficient poling.[17, 19, 39] We also synthesized **BTP** variants for exploring relative substitution effects on the donor linkage (**STP1**), bridge (**BTF1**), and secondary electron-donating groups (**BTH1**). These structures, along with a summary of the computational screening data are shown in Figure 1.

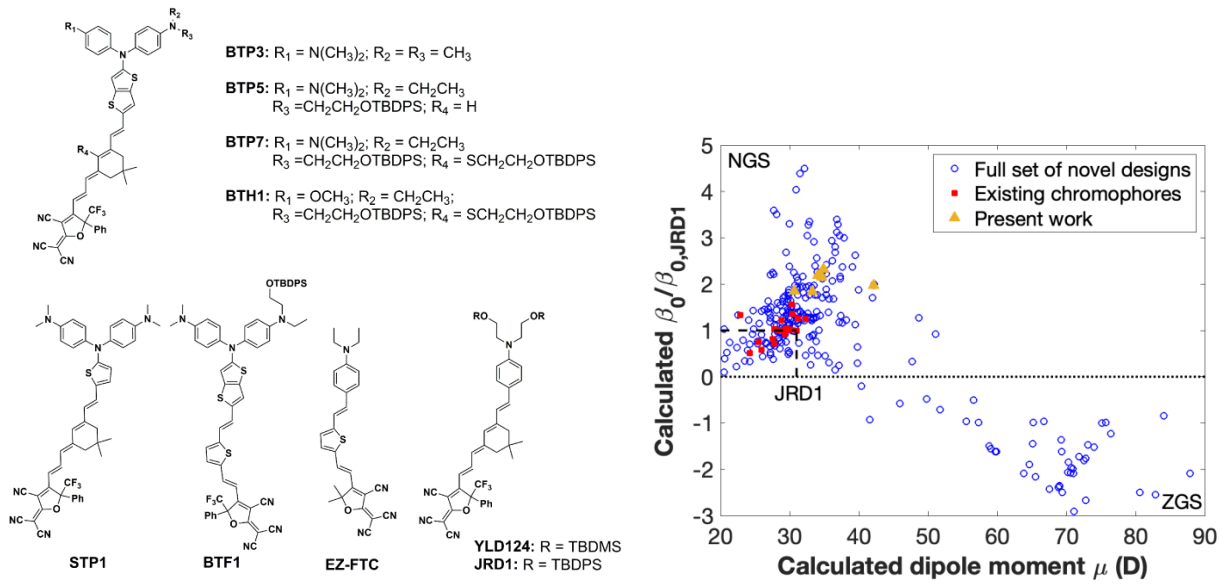

Figure 1. Novel bis(4-dialkylaminophenyl)heteroarylamino chromophores **BTP3**, **BTP5**, **BTP7**, **BTF1, BTH1**, and **STP1** as well as reference molecules **JRD1, YLD124** and **EZ-FTC**. (left) TBDPS is *tert*-butydiphenylsilyl. TBDMS is *tert*-butyldimethylsilyl. The novel chromophores are highlighted in gold on a plot of predicted hyperpolarizability vs **JRD1** as a function of dipole moment (right); all of the chromophores show a substantial increase in predicted hyperpolarizability versus existing chromophores with little to no increase in dipole moment except for the thiophene-linked chromophore **STP1**. Groupings associated with neutral ground state (NGS) and zwitterionic ground state (ZGS) chromophores are noted. The dashed lines indicate the computed hyperpolarizability and dipole moment of **JRD1**.

The above chromophores were synthesized and were characterized in solution by femtosecond hyper-Rayleigh scattering (HRS) to determine their hyperpolarizabilities.[40-42] We also characterized the linear optical properties, thermodynamic properties, optical constants, and bulk EO performance of the chromophores as a function of concentration in a poly(methylmethacrylate) (PMMA) host by the Teng-Man simple reflection method.[43, 44]

We measured dramatically enhanced static molecular hyperpolarizabilities by HRS in chloroform (solution) for the new bis(4-dialkylaminophenyl)heteroarylamino chromophores compared with reference chromophores **JRD1**, which has the highest EO activity reported in the EO literature,[4, 17] and **EZ-FTC,** which is a well-known EO reference compound (Table 1).[45] Hyperpolarizabilities are reported as $\beta_{zzz,0}$, which refers to the component of the hyperpolarizability along the dipole axis (z-axis) in the zero-frequency limit. All of the novel chromophores outperform reference chromophore **JRD1**, with the strongest performance observed for chromophores with a ring-locked polyene bridge and a thienothiophene-containing bis(4-dialkylaminophenyl)amine donor. Performance was only slightly reduced when using a thiophene-containing (**FTC**-like) bridge (**BTF1**) or replacing one dialkylamino group in the donor with a methoxy group (**BTH1**). The highest hyperpolarizability was obtained with **BTP7**, having a more than 3-fold improvement in molecular hyperpolarizability compared with **JRD1,** and exceeding the highest static hyperpolarizability previously reported in the literature by more than a factor of two (Compound **1** in Cheng et al. 2008)[46] when adjusting for wavelength and reference standard (See Table S6, ESI†). The performance of all chromophores also exceeded that of several chromophores with strong julolidine donor moieties, labeled as **ZH-1** and molecule **3** in Table 1.[47, 48] Cyclic

voltammetry in dichloromethane was used to estimate the HOMO energy levels of the new compounds (Figure 2b). Higher HOMO energy levels are expected for stronger electron donor compounds, and the bis(4-dialkylaminophenyl)amine compounds have a significantly higher (by 0.4 - 0.32 eV) HOMO levels than dialkylamine donor compound **JRD1** and 0.16 eV higher HOMO than julolidine donor compounds on average (Table S5, ESI†). LUMO values experienced much smaller shifts due to the novel chromophores and reference molecules sharing the same acceptor moieties. Absorbance spectroscopy was used to estimate chromophore band gaps, and band gap was found to correlate very well with both measured and calculated hyperpolarizability (Figures S24-S28, ESI†). Band gaps for the bis(4-dialkylaminophenyl)amino thienothiophene chromophores (0.81-0.86 eV) were slightly smaller than the bis(4-dialkylaminophenyl)amino thiophene chromophore and the mono(4-dialkylaminophenyl)amino thienothiophene chromophore (0.91-0.95 eV), and significantly smaller than **JRD1** (1.09 eV).

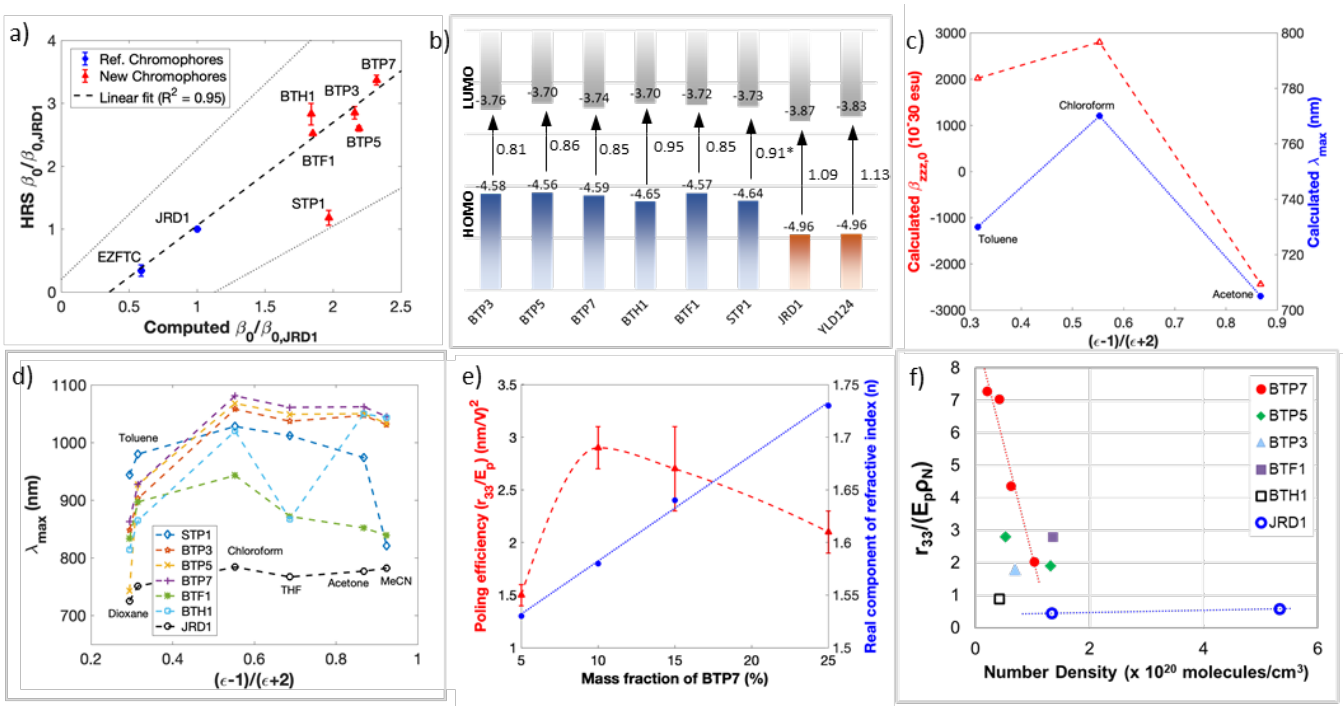

Figure 2. a) Comparison of DFT (M062X/6-31+G(d)) and experimental (femtosecond HRS) hyperpolarizabilities in chloroform solution. HRS data was extrapolated to zero frequency using the damped two-level model; data analysis is discussed in ESI†. **STP1** is excluded from the fit as an outlier. The dashed line indicates the linear fit and the dotted lines indicate the 95% confidence interval of the fit. b) HOMO (cyclic voltammetry) and LUMO energy levels and thin film optical energy gaps, in eV; LUMO = HOMO (CV) + Band gap (optical). **STP1** optical energy gap estimated as described in ESI†. c) Solvatochromism in computational $\beta_{zzz,0}$ and λ_{max} for **STP1**. The dotted or dashed lines are a guide to the eye. d) λ_{max} vs. solvent polarity on the Reichardt scale ($(\epsilon-1)/(\epsilon+2)$) spanning a range of dielectric constants from 1,4-dioxane (ϵ=2.2) to acetonitrile (ϵ=37.5). The dashed lines are a guide to the eye. e) Poling efficiency and refractive index curves for **BTP7** in PMMA. The blue, dotted line represents a least-squares linear regression, the red, dashed line is a cubic spline interpolation. f) Poling efficiencies per number density of chromophores in PMMA and neat **JRD1**.

A comparison of experimental and computed hyperpolarizabilities is shown in Figure 2a. A strong correlation is observed, with only the thiophene-containing chromophore **STP1** showing a significant deviation. The discrepancy was consistent with a significantly larger hypsochromic shift of its principal intramolecular charge transport band (λ_{max}) in polar solvents (Figure S15a, ESI†), indicating that it is likely close to a low-β cyanine-like state in chloroform solution.[27, 49] These results were confirmed by computational studies from low dielectric (toluene ϵ=2.4) to high dielectric (acetone ϵ=20.7) environments, in which **STP1** undergoes a dramatic increase in dipole moment, hyperpolarizability sign reversal, and directional reversal of solvatochromism (Figures 2c-2d); these are characteristic properties of a transition from a neutral ground state (NGS) to a cyanine state to a zwitterionic ground state (ZGS). The deviation from the otherwise high correlation between DFT and experiment is likely due to the rapid change in β with reaction field strength near the cyanine limit, where β is strongly dependent on degree of ground-state polarization and systematic errors in the solvent reaction field model would lead to large errors in β. In contrast to **STP1** in high dielectric environments, the hyperpolarizability for **BTP** chromophores does not become negative, but remains relatively flat (experimentally decreases slightly, computationally increases slightly (Figures 2c, S22, S23 and Tables S5-S11, ESI†). Absorbance solvatochromism measurements show that all of the novel chromophores had stronger solvatochromism than **JRD1**, but only **STP1** and **BTF1** had a strong negative solvatochromism in high dielectric environments (Figure 2d), suggesting that in high dielectric solvents, the **BTP** and **BTH** chromophores become cyanine-like, but not zwitterionic like **STP1** and **BTF1**. While we cannot completely eliminate the possibility that the solvent-dependent behavior is not a function of specific solvent-chromophore interactions, we believe that the small degree of solvatochromism for **JRD1** compared to the other novel chromophores indicates that solvent-chromophore interactions aren't dominating the observed effects. Calculations and experimental measurements of the CN stretch frequencies by FTIR as a function of solvent dielectric also support cyanine-like or ZGS behavior of **BTP** and **STP1** chromophores compared to **JRD1** (Figures S40, S41, S66, ESI†).

Table 1. Linear and nonlinear optical properties of chromophores.

Name	β_{zzz} (1300 nm)[a]	$\beta_{zzz,0}$	$\beta_{zzz,0}/\beta_{zzz,0,JRD1}$	Comp[b]. $\beta_0/\beta_{0,JRD1}$	λ_{max} (nm) $CHCl_3$	λ_{max} (nm) Film	n_{1310}	n_{1550}
JRD1	3330 ± 50	1060 ± 20	1 ± 0.02	1	790	800	1.91	1.85
EZFTC	3600 ± 900	360 ± 90	0.34 ± 0.09	0.59	676	678	1.95	1.91
BTP3	4880 ± 170	3030 ± 100	2.85 ± 0.10	2.16	1055	1105	2.78	2.39
BTP5	4410 ± 70	2740 ± 40	2.60 ± 0.04	2.19	1070	1103	2.61	2.32
BTF1	4750 ± 20	2650 ± 10	2.52 ± 0.01	1.85	950	951	2.20	2.06
BTP7	5720 ± 130	3550 ± 80	3.37 ± 0.08	2.32	1081	1114	2.29	2.07
STP1	2000 ± 210	1250 ± 130	1.18 ± 0.12	1.97	1030	-	-	-
BTH1	4900 ± 300	3000 ± 200	2.83 ± 0.17	1.76	1020	1097	2.09	1.89
ZH-1[47]				1.24	763			
3[48]				1.03	980	1250		

[a]HRS – femtosecond HRS at 1300 nm in $CHCl_3$, extrapolation to zero frequency using damped TLM (0.1 eV linewidth). Hyperpolarizabilities in 10^{-30} esu. Reference against solvent ($CHCl_3$, using Campo et al 2009 value of $\beta_{zzz,0} \sim 0.44 \times 10^{-30}$ esu).[42] [b]Computational predictions – M062X/6-31+G(d) in PCM $CHCl_3$ at zero frequency, analytic differentiation, 2-carbon truncation on inactive side chains.

The refractive index (*n*) of unpoled films of neat chromophores and chromophore/PMMA blends was measured using variable angle spectroscopic ellipsometry (VASE) and is summarized in Table 1 and Table S2 (ESI†). Solubility of **STP1** was insufficient to form a

measurable film. Greatly enhanced refractive index values were observed for neat films of bis(4-dialkylaminophenyl)amino thienophene-type chromophores at two of the important telecom wavelengths (1310 nm and 1550 nm), which present a potential route for improving the device performance, as the voltage-length product $V_{\pi}L$ is inversely proportional to $n^3 r_{33}$. **BTP3** films have a larger number of chromophores per unit volume (6.96 x 10^{20} molecules/cm^3, assuming a density of 1 g/cm^3) and exhibit a refractive index of $n_{1310} = 2.78$ ($n_{1550} = 2.39$), which is one of the highest reported for organic EO materials to date, and is higher than that of lithium niobate ($n_{1310} = 2.22$). However, **BTP3** is a poor film former, likely due to its large dipole moment (see ESI†) combined with its lack of bulky and conformationally flexible pendant groups. The introduction of bulky groups such as TBDPS can increase solubility and film-forming ability and improve the acentric order parameter, $\langle \cos^3\theta \rangle$, in electric field poled films by inhibiting dipole-dipole interactions.[17] Neat **BTP5** and **BTP7** have good solubility and film formation properties, and an acceptable reduction in number density (ρ_N) and n proportional to the amount of added steric bulk. The neat chromophore films exhibited strong absorption at 1310 nm (Table S2, ESI†), potentially leading to unacceptable optical loss in nanophotonic devices. However, **BTP**-type chromophores are well suited to blending with polymer hosts, showing large EO activity at low concentration (~10 wt%). Optical loss is greatly reduced at these low concentrations, enabling use in nanophotonic EO devices. In present nanophotonic devices, insertion loss is typically dominated by coupling loss,[9, 50] and the propagation component of the insertion loss is dominated by the narrow slot waveguides. State-of-the-art POH devices using neat **JRD1** as the OEO material have propagation losses in the 0.2-0.4 dB/μm range,[50] and state-of-the art SOH devices have propagation losses of approximately 2.5 dB/mm.[9] To be acceptable, a material should have a propagation loss that does not exceed present waveguide losses. State of the art waveguide loss values imply a threshold for k at 1550 nm of 0.0055 for POH and 0.00007 for SOH. All of the new compounds are within the POH threshold for at least one concentration tested, and most compare favorably to conventional guest-host system 25% **YLD124** in PMMA (Table S2, ESI†).

Table 2. Electric Field Poling Data for EO Chromophores in Bulk Devices

wt % Chromophore in PMMA	ρ_N [a]	r_{33}/E_p (nm^2/V^2)[b]	$r_{33}/(E_p\rho_N)$[c]	max. r_{33} (pm/V)
10% **BTP3**	0.696	1.8±0.2	2.6±0.3	150±20
10% **BTP5**	0.525	2.8±0.2	5.3±0.4	280±20
25% **BTP5**	1.31	1.9±0.2	1.5±0.2	120±10
5% **BTP7**	0.206	1.5±0.1	7.3±0.5	100±10
10% **BTP7**	0.412	2.9±0.2	7.0±0.5	270±40
15% **BTP7**	0.618	2.7±0.4	4.4±0.6	240±40
25% **BTP7**	1.03	2.1±0.2	2.1±0.2	180±20
25% **BTF1**	1.36	2.8±0.2	2.1±0.1	240±20
10% **BTH1**	0.416	0.9±0.1	2.2±0.2	88±6
35%**AJLZ55** [48]	2.24	2.18	0.97	218
25% **1**[46]	2.12	1.82	0.86	219
47% **10**[51]	2.94	3.3	1.1	262
30% **6**+**24**[52]	3.05	5.6	1.84	387
25% **JRD1**	1.33	0.6	0.45	72.5
100% **JRD1**	5.33	3.1±0.1	0.58±0.02	343±60

[a]Number density (assumes mass density of 1 g/cm^3). [b]Results from multiple poling experiments (Figure S19, ESI†). All reported results are in the absence of charge-blocking layers. [c]Poling efficiency per number density ($nm^2/V^2/(10^{20}$ molecules $cm^{-3})$).

EO performance was measured for the novel chromophores dispersed in a PMMA host; leakage current for neat chromophore films was too high to allow effective poling as neat materials (even when using charge barrier layers such as TiO_2 or benzocyclobutene polymer[17]. Parallel plate bulk devices for EO measurements were prepared by spin coating thin films of chromophore-polymer composites on ITO substrates followed by sputter-coating gold top electrodes. Poling was performed at approximately 115°C using a DC poling field (E_p) in the 20 to 110 V/μm range. Results of EO measurements at 1310 nm are shown in Table 2 and Figure S19 (ESI†). Poling efficiencies r_{33}/E_p were determined by linear fitting of the electro-optic activity (in pm/V) versus E_p. All chromophore composites showed exceptional performance at low to moderate concentration, with poling efficiencies per number density ($r_{33}/(\rho_N E_p)$) > 3x that of **JRD1**. **BTP7** at 10 wt% concentration showed the highest performance, with a poling efficiency of 2.9 ± 0.2 nm^2/V^2, competitive with neat **JRD1**, which has a poling efficiency of 3.1 ± 0.1 nm^2/V^2 in an identical device architecture.[17, 53] Generally, the maximum r_{33} is achieved at 15-40 wt% chromophore in polymer. The optimal concentration depends on the chromophore hyperpolarizability, dipole moment, molecular shape (e.g. ellipsoid), site isolation side chains, polymer miscibility etc., and thus varies from chromophore to chromophore. A high β chromophore achieving a maximum r_{33} at 10 wt% and achieving such a high r_{33} and poling efficiency (r_{33}/E_p) at 10 wt% are surprising and exceptional. This is best borne out by highlighting that the poling efficiency per number density of 10 wt% **BTP7** is 12.1 ± 0.8 that of neat **JRD1**, suggesting highly efficient poling combined with the exceptional hyperpolarizability of **BTP7**. Applying the damped two-level model (see ESI†) suggests that the **BTP7** resonance-corrected Pockels effect hyperpolarizability $\beta(-\omega,\omega,0)$ at 1310 nm in the thin film environment is 10.2 ± 0.2 times that of **JRD1**, such that most of the enhancement in EO performance is due to the large hyperpolarizability, with the balance likely due to improved ordering

due to the presence of the bulky and flexible side chains, which was previously observed with **HLD**.[19] Performance for **BTP7** declined as chromophore concentration increased past 10 wt% (Figure 2e). **BTP5** exhibited a similar trend and nearly matched **BTP7** in performance. The similar EO performance between **BTP5** and **BTP7** but greater performance of **BTP7** per unit concentration suggests that it orders more efficiently than **BTP5**, consistent with order-number density tradeoffs observed from prior modeling of chromophores with different configurations of bulky groups.[39] **BTP3** exhibited lower overall performance and chromophore concentration could not be easily increased due to poor solubility. **BTF1**, with lower hyperpolarizability and less resonance enhancement, showed excellent performance at 25 % concentration. **BTH1** showed the lowest performance but still exceeded **JRD1** on a poling efficiency per-concentration basis. The large improvement in EO activity at a given concentration in a polymer host demonstrates the utility of the chromophores in the thienothiophene-derived donor class, such as **BTP5**, **BTP7** and **BTF1** (Figure 2f)**.** $r_{33}/(\rho_N E_p)$ is reported for other literature chromophores that have excellent r_{33} values as guest/host systems in Table 2. However, despite their exceptional r_{33} values, the $r_{33}/(\rho_N E_p)$ values are ~4-7 times lower than our best example (**BTP7**), which further illustrates the novelty of this new class of chromophores. The novel **BT**x family of chromophores can deliver high device performance while providing substantial flexibility for blending with polymers for controlling mechanical and thermal properties and a wide range of refractive index tuning.

Conclusions

In conclusion, a new series of second-order NLO chromophores with record hyperpolarizabilities was synthesized based on computationally-driven designs and characterized. The highlight of the present work is the highly enhanced molecular hyperpolarizability of chromophore **BTP7**, which represents a 3.4-fold increase of $\beta_{zzz,0}$ over chromophore **JRD1** while keeping the dipole moment within a range conducive to processing into high-quality films. Meanwhile, the electric field poled films of 10 wt% **BTP7** in PMMA displayed a much higher poling efficiency (2.9 ± 0.2 nm^2/V^2) than 25 wt% **JRD1** in PMMA (0.6 nm^2/V^2) and comparable to neat **JRD1**, reflecting a 12-fold improvement in poling efficiency on a per-chromophore basis. These results demonstrate the predictive power of quantum mechanical calculations for assessing hyperpolarizability of high-performance chromophores and suggest that higher molecular-level nonlinearity can be obtained in OEO materials without excessively compromising processability or stability, which could lead to even higher performance organic EO materials for applications in nanophotonic devices.

Author Contributions

LEJ, DLE, and BHR conceived the project. LEJ performed electronic structure calculations and associated data analysis. LEJ, DLE, HX, and BHR contributed to design of novel compounds. HX synthesized and performed structural, linear optical, electro-optic, and thermal characterization on all compounds. DLE performed electrochemical and IR spectroscopic characterization and assisted with other techniques. and DLE and SRH contributed characterization protocols and assisted with interpretation of data. YdC performed all Hyper-Rayleigh Scattering spectroscopy experiments and associated data analysis; KC and LEJ assisted with HRS data interpretation. HX, LEJ, and DLE wrote the initial manuscript and led revision in response to reviewer comments. LEJ and DLE managed the project. BHR, LRD, and KC provided research-group level supervision, mentoring, and funding. All authors edited and approved the manuscript.

Conflicts of interest

Competing Financial Interest Disclosure. Some work in this study is related to technology described in patent applications filed by the University of Washington, "Organic Electro-Optic Chromophores," US Provisional Applications No. 62/911,067 and 62/934,398, which have been licensed by Nonlinear Materials Corporation (NLM). L.E.J. is a co-founder and part-time employee of NLM and an equity holder in NLM. S.R.H is a part-time employee of NLM and equity holder in NLM. D.L.E. and B.H.R. are equity holders in NLM and advisors to NLM. The terms of this arrangement have been reviewed and approved by the University of Washington in accordance with its policies governing outside work and financial conflicts of interest in research.

Acknowledgements

We gratefully acknowledge the financial support of the Air Force Office of Scientific Research (FA9550-19-1-0069), the University of Washington College of Arts and Sciences, Flemish Fund for Scientific Research (FWO-V, G0A1817N), and from the University of Leuven (C16/16/003). Part of this work was conducted at the Molecular Analysis Facility, a National Nanotechnology Coordinated Infrastructure (NNCI) site at the University of Washington, which is supported in part by funds from the National Science Foundation (awards NNCI-2025489, NNCI-1542101), the Molecular Engineering & Sciences Institute, and the Clean Energy Institute. We also thank Drs. Stephanie J. Benight and Philip A. Sullivan for useful discussion, as well as prior synthetic work by Drs. Joshua A. Davies and Nathan P. Sylvain and HRS work by Dr. Denise Bale that suggested the potential of triarylamine donors for substantial enhancement in hyperpolarizability.

Notes and references

1. M. Ayata, Y. Fedoryshyn, W. Heni, B. Baeuerle, A. Josten, M. Zahner, U. Koch, Y. Salamin, C. Hoessbacher, C. Haffner, D. L. Elder, L. R. Dalton and J. Leuthold, *Science*, 2017, **358**, 630-632.
2. W. Heni, Y. Kutuvantavida, C. Haffner, H. Zwickel, C. Kieninger, S. Wolf, M. Lauermann, Y. Fedoryshyn, A. F. Tillack and L. E. Johnson, *ACS Photonics*, 2017, **4**, 1576-1590.
3. C. Haffner, D. Chelladurai, Y. Fedoryshyn, A. Josten, B. Baeuerle, W. Heni, T. Watanabe, T. Cui, B. Cheng, S. Saha, D. L. Elder, L. R. Dalton, A. Boltasseva, V. M. Shalaev, N. Kinsey and J. Leuthold, *Nature*, 2018, **556**, 483-486.
4. C. Kieninger, Y. Kutuvantavida, D. L. Elder, S. Wolf, H. Zwickel, M. Blaicher, J. N. Kemal, M. Lauermann, S. Randel, W. Freude, L. R. Dalton and C. Koos, *Optica*, 2018, **5**, 739-748.
5. M. Burla, C. Hoessbacher, W. Heni, C. Haffner, Y. Fedoryshyn, D. Werner, T. Watanabe, H. Massler, D. L. Elder and L. R. Dalton, *APL Photonics*, 2019, **4**, 056106.
6. I.-C. Benea-Chelmus, Y. Salamin, F. F. Settembrini, Y. Fedoryshyn, W. Heni, D. L. Elder, L. R. Dalton, J. Leuthold and J. Faist, *Optica*, 2020, **7**, 498-505.
7. U. Koch, C. Uhl, H. Hettrich, Y. Fedoryshyn, C. Hoessbacher, W. Heni, B. Baeuerle, B. I. Bitachon, A. Josten, M. Ayata, H. Xu, D. L. Elder, L. R. Dalton, E. Mentovich, P. Bakopoulos, S. Lischke, A. Krüger, L. Zimmermann, D. Tsiokos, N. Pleros, M. Möller and J. Leuthold, *Nat. Electron.*, 2020, **3**, 338-345.
8. B. Baeuerle, C. Hoessbacher, W. Heni, Y. Fedoryshyn, U. Koch, A. Josten, D. L. Elder, L. R. Dalton and J. Leuthold, *Opt Express*, 2020, **28**, 8601-8608.
9. C. Kieninger, C. Fullner, H. Zwickel, Y. Kutuvantavida, J. N. Kemal, C. Eschenbaum, D. L. Elder, L. R. Dalton, W. Freude, S. Randel and C. Koos, *Opt Express*, 2020, **28**, 24693-24707.

10. W. Heni, Y. Fedoryshyn, B. Baeuerle, A. Josten, C. B. Hoessbacher, A. Messner, C. Haffner, T. Watanabe, Y. Salamin, U. Koch, D. L. Elder, L. R. Dalton and J. Leuthold, *Nat. Commun.*, 2019, **10**, 1694.
11. Y. Salamin, I.-C. Benea-Chelmus, Y. Fedoryshyn, W. Heni, D. L. Elder, L. R. Dalton, J. Faist and J. Leuthold, *Nat. Commun.*, 2019, **10**, 5550.
12. W. Heni, B. Baeuerle, H. Mardoyan, F. Jorge, J. M. Estaran, A. Konczykowska, M. Riet, B. Duval, V. Nodjiadjim, M. Goix, J. Dupuy, M. Destraz, C. Hoessbacher, Y. Fedoryshyn, H. Xu, D. L. Elder, L. Dalton, J. Renaudier and J. Leuthold, *J. Lightwave Technol.*, 2020, DOI: 10.1109/JLT.2020.2972637, 1-1.
13. R. Bonjour, M. Burla, F. C. Abrecht, S. Welschen, C. Hoessbacher, W. Heni, S. A. Gebrewold, B. Baeuerle, A. Josten, Y. Salamin, C. Haffner, P. V. Johnston, D. L. Elder, P. Leuchtmann, D. Hillerkuss, Y. Fedoryshyn, L. R. Dalton, C. Hafner and J. Leuthold, *Opt. Express.*, 2016, **24**, 25608-25618.
14. C. Koos, J. Leuthold, W. Freude, M. Kohl, L. Dalton, W. Bogaerts, A. L. Giesecke, M. Lauermann, A. Melikyan and S. Koeber, *J. Lightwave Technol.*, 2016, **34**, 256-268.
15. S. Ummethala, T. Harter, K. Koehnle, Z. Li, S. Muehlbrandt, Y. Kutuvantavida, J. Kemal, P. Marin-Palomo, J. Schaefer, A. Tessmann, S. K. Garlapati, A. Bacher, L. Hahn, M. Walther, T. Zwick, S. Randel, W. Freude and C. Koos, *Nat. Photonics.*, 2019, **13**, 519-524.
16. C. Haffner, W. Heni, Y. Fedoryshyn, J. Niegemann, A. Melikyan, D. L. Elder, B. Baeuerle, Y. Salamin, A. Josten and U. Koch, *Nat. Photonics.*, 2015, **9**, 525.
17. W. Jin, P. V. Johnston, D. L. Elder, A. F. Tillack, B. C. Olbricht, J. Song, P. J. Reid, R. Xu, B. H. Robinson and L. R. Dalton, *Appl. Phys. Lett.*, 2014, **104**, 243304-243304-243305.
18. D. L. Elder, C. Haffner, W. Heni, Y. Fedoryshyn, K. E. Garrett, L. E. Johnson, R. A. Campbell, J. D. Avila, B. H. Robinson, J. Leuthold and L. R. Dalton, *Chem. Mater.*, 2017, **29**, 6457-6471.
19. H. J. Xu, F. G. Liu, D. L. Elder, L. E. Johnson, Y. de Coene, K. Clays, B. H. Robinson and L. R. Dalton, *Chem. Mater.*, 2020, **32**, 1408-1421.
20. S. Wolf, H. Zwickel, W. Hartmann, M. Lauermann, Y. Kutuvantavida, C. Kieninger, L. Altenhain, R. Schmid, J. Luo, A. K. Jen, S. Randel, W. Freude and C. Koos, *Sci. Rep.*, 2018, **8**, 2598.
21. S. Koeber, R. Palmer, M. Lauermann, W. Heni, D. L. Elder, D. Korn, M. Woessner, L. Alloatti, S. Koenig and P. C. Schindler, *Light-Sci Appl.*, 2015, **4**, e255.
22. L. R. Dalton, P. A. Sullivan and D. H. Bale, *Chem. Rev.*, 2010, **110**, 25-55.
23. J. Wu, J. Luo and A. K.-Y. Jen, *J. Mater. Chem. C*, 2020, **8**, 15009-15026.
24. L. R. Dalton, S. J. Benight, L. E. Johnson, D. B. Knorr, I. Kosilkin, B. E. Eichinger, B. H. Robinson, A. K.-Y. Jen and R. M. Overney, *Chem. Mater.*, 2011, **23**, 430-445.
25. B. Robinson, L. Johnson, D. Elder, A. Kocherzhenko, C. Isborn, C. Haffner, W. Heni, C. Hoessbacher, Y. Fedoryshyn and Y. Salamin, *J. Lightwave Technol.*, 2018, **36**, 5036-5047.
26. L. E. Johnson, L. R. Dalton and B. H. Robinson, *Acc. Chem. Res.*, 2014, **47**, 3258-3265.
27. J. A. Davies, A. Elangovan, P. A. Sullivan, B. C. Olbricht, D. H. Bale, T. R. Ewy, C. M. Isborn, B. E. Eichinger, B. H. Robinson, P. J. Reid, X. Li and L. R. Dalton, *J. Am. Chem. Soc.*, 2008, **130**, 10565-10575.
28. Y.-J. Cheng, J. Luo, S. Hau, D. H. Bale, T.-D. Kim, Z. Shi, D. B. Lao, N. M. Tucker, Y. Tian, L. R. Dalton, P. J. Reid and A. K.-Y. Jen, *Chem. Mater.*, 2007, **19**, 1154-1163.
29. P. A. Sullivan, H. Rommel, Y. Liao, B. C. Olbricht, A. J. Akelaitis, K. A. Firestone, J.-W. Kang, J. Luo, J. A. Davies and D. H. Choi, *J. Am. Chem. Soc.*, 2007, **129**, 7523-7530.
30. H. Xu, D. L. Elder, L. E. Johnson, B. H. Robinson and L. R. Dalton, *ACS Appl. Mater. Interfaces*, 2019, **11**, 21058-21068.
31. X. Zang, G. Liu, Q. Li, Z. a. Li and Z. Li, *Macromolecules*, 2020, **53**, 4012-4021.
32. X. Zang, H. Liu, Q. Li, Z. a. Li and Z. Li, *Polym Chem.*, 2020, **11**, 5493-5499.
33. T. D. Kim, J. W. Kang, J. D. Luo, S. H. Jang, J. W. Ka, N. Tucker, J. B. Benedict, L. R. Dalton, T. Gray, R. M. Overney, D. H. Park, W. N. Herman and A. K.-Y. Jen, *J. Am. Chem. Soc.*, 2007, **129**, 488-489.

34. D. L. Elder, S. J. Benight, J. Song, B. H. Robinson and L. R. Dalton, *Chem. Mater.*, 2014, **26**, 872-874.
35. J. Wu, B. Wu, W. Wang, K. S. Chiang, A. K.-Y. Jen and J. Luo, *Mater. Chem. Front*, 2018, **2**, 901-909.
36. G. Bourhill, J.-L. Bredas, L.-T. Cheng, S. R. Marder, F. Meyers, J. W. Perry and B. G. Tiemann, *J. Am. Chem. Soc.*, 1994, **116**, 2619-2620.
37. L. Johnson, H. Xu, Y. de Coene, D. Elder, K. Clays, L. Dalton and B. Robinson, *Next-generation materials for hybrid electro-optic systems (Conference Presentation)*, SPIE, 2019.
38. L. Johnson, H. Xu, S. Hammond, D. Elder, S. Benight, Y. de Coene, J. Hesse-Withbroe, K. Clays, L. Dalton and B. Robinson, *Advances in high-performance hybrid electro-optics*, SPIE, 2020.
39. A. F. Tillack and B. H. Robinson, *JOSA B*, 2016, **33**, E121-E129.
40. K. Clays and A. Persoons, *Phys. Rev. Lett.*, 1991, **66**, 2980-2983.
41. K. Clays and A. Persoons, *Rev. Sci. Instrum.*, 1992, **63**, 3285-3289.
42. J. Campo, F. Desmet, W. Wenseleers and E. Goovaerts, *Opt. Express.*, 2009, **17**, 4587-4604.
43. C. C. Teng and H. T. Man, *Appl. Phys. Lett.*, 1990, **56**, 1734-1736.
44. Y. Shuto and M. Amano, *J. Appl. Phys.*, 1995, **77**, 4632-4638.
45. M. Q. He, T. M. Leslie and J. A. Sinicropi, *Chem. Mater.*, 2002, **14**, 4662-4668.
46. Y. J. Cheng, J. D. Luo, S. Huang, X. H. Zhou, Z. W. Shi, T. D. Kim, D. H. Bale, S. Takahashi, A. Yick, B. M. Polishak, S. H. Jang, L. R. Dalton, P. J. Reid, W. H. Steier and A. K.-Y. Jen, *Chem. Mater.*, 2008, **20**, 5047-5054.
47. H. Zhang, F. Huo, F. Liu, Z. Chen, J. Liu, S. Bo, Z. Zhen and L. Qiu, *RSC Adv.*, 2016, **6**, 99743-99751.
48. X.-H. Zhou, J. Luo, J. A. Davies, S. Huang and A. K.-Y. Jen, *J. Mater. Chem.*, 2012, **22**, 16390-16398.
49. S. R. Marder, C. B. Gorman, B. G. Tiemann, J. W. Perry, G. Bourhill and K. Mansour, *Science*, 1993, **261**, 186.
50. W. Heni, C. Haffner, D. L. Elder, A. F. Tillack, Y. Fedoryshyn, R. Cottier, Y. Salamin, C. Hoessbacher, U. Koch and B. Cheng, *Opt. Express.*, 2017, **25**, 2627-2653.
51. J. Luo, Y.-J. Cheng, T.-D. Kim, S. Hau, S.-H. Jang, Z. Shi, X.-H. Zhou and A. K.-Y. Jen, *Org. Lett.*, 2006, **8**, 1387-1390.
52. T. D. Kim, J. D. Luo, Y. J. Cheng, Z. W. Shi, S. Hau, S. H. Jang, X. H. Zhou, Y. Tian, B. Polishak, S. Huang, H. Ma, L. R. Dalton and A. K.-Y. Jen, *J. Phys. Chem. C*, 2008, **112**, 8091-8098.
53. W. W. Jin, P. V. Johnston, D. L. Elder, K. T. Manner, K. E. Garrett, W. Kaminsky, R. M. Xu, B. H. Robinson and L. R. Dalton, *J. Mater. Chem. C*, 2016, **4**, 3119-3124.